

Document downloaded from:

<http://hdl.handle.net/10251/197448>

This paper must be cited as:

Gibouin, F.; Van Der Sman, R.; Benedito Fort, JJ.; Della Valle, G. (2022). Rheological properties of artificial boluses of cereal foods enriched with legume proteins. *Food Hydrocolloids*. 122:1-10. <https://doi.org/10.1016/j.foodhyd.2021.107096>



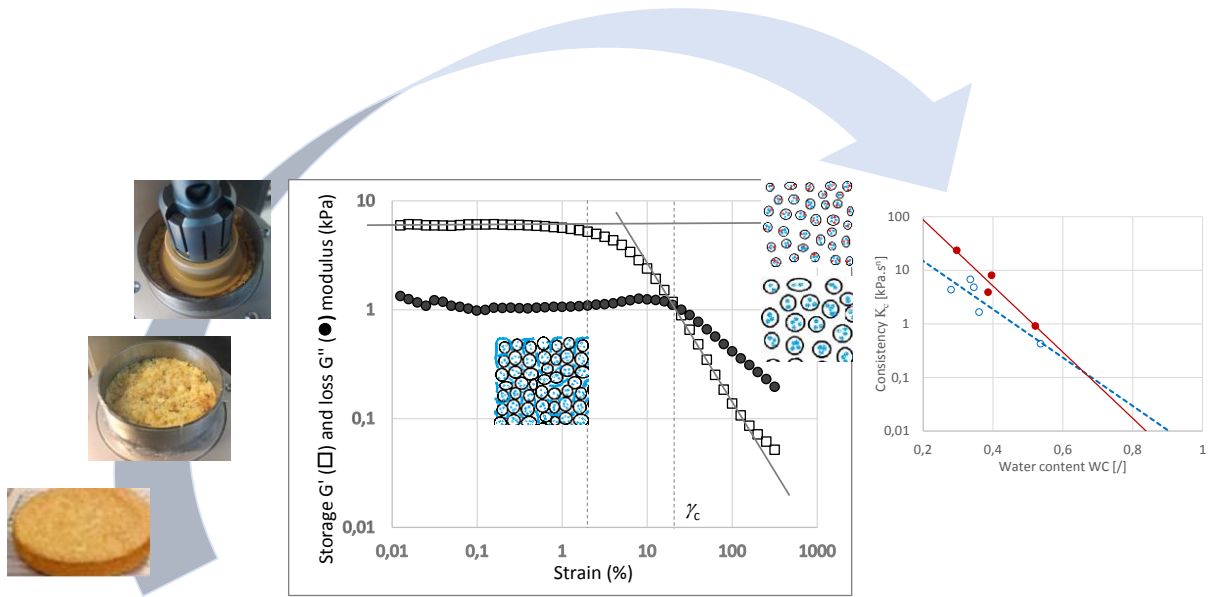
The final publication is available at

<https://doi.org/10.1016/j.foodhyd.2021.107096>

Copyright Elsevier

Additional Information

- Rheological properties of artificial food boluses are determined in FOP conditions
- Cereal foods bolus behave like a gel, destructured for a characteristic stress τ_c
- A food/water interaction coefficient α is derived from τ_c variations with water
- Cereal foods bolus can be considered as a suspension of soft swollen particles
- For flow properties, α values are increased when adding protein to the food



Cereal food (sponge cake) is ground and hydrated before testing on rheometer to determine the flow transition (here by strain sweep) of the suspension of swollen soft particles (inserted sketches) and the influence of protein addition (symbolized in red) on plasticization by water, is reflected by the variations of bolus consistency with water.

1 **Rheological properties of artificial boluses of cereal foods enriched with legume proteins**

2 F. Gibouin¹, R. van der Sman², J. Benedito³, G. Della Valle^{1*}

3 ¹ *INRAE UR-1268 Biopolymères Interactions et Assemblages, 44316 Nantes, France*

4 ² *Agrotechnology and Food Sciences, Wageningen University and Research, 6708 WG Wageningen,*
5 *The Netherlands*

6 ³ *Universitat Politècnica de Valencia, Departamento de Tecnología de Alimentos, 46071, Valencia,*
7 *Spain*

8 * corresponding author: guy.della-valle@inrae.fr

9 **Abstract**

10 The properties of artificial food bolus are studied by dynamic oscillatory and capillary
11 rheometry as functions of bolus water content, in the usual range of saliva hydration, for four cereal
12 products: sponge cake, extruded flat bread and their counterpart enriched in legume proteins. All
13 boluses followed the same rheological behaviour characterised by (1) solid -like in the linear
14 viscoelastic domain and (2) Herschel-Bulkley model for large shear strain. Hence, four characteristic
15 rheological properties are determined: modulus at viscoelastic plateau, characteristic stress at
16 transition to flow, yield stress and consistency in the flow regime. Water content considerably
17 decreased these properties according to an exponential decay, which allowed determining
18 interactions coefficients ($5 \leq \alpha \leq 30$). These values are of the same order of magnitude as the
19 plasticization coefficient of starch by water. They were larger for the extruded pea based (EFP, $\alpha \geq$
20 15), and were lower for the sponge cake (SC, $\alpha \leq 15$). The variations for the different rheological
21 properties are discussed in terms of matter state, envisioning bolus as a suspension of soft swellable
22 particles. The comparison of these values with those encountered for real boluses from similar foods
23 suggests that these results contribute to define a coefficient of interaction of food with saliva.

24

25

26 **Keywords:** Herschel-Bulkley model; interaction coefficient; modulus; plant protein; viscosity

27

28

29 **Nomenclature**

30	a	shift factor used to derive the flow master curve
31	D, D_p	diameters of rheometer capillary die and piston, respectively
32	EF, EFP	extruded flat bread end extruded pea based snack, respectively
33	G', G'', G^*	storage, dissipative and complex modulus, respectively
34	G'_0	theoretical value of storage modulus for dry bolus
35	K, K_c	consistency and its corrected value in the Herschel-Bulkley model
36	K_{c0}	theoretical value of consistency for the dry bolus
37	L/D	length to diameter capillary die ratio
38	n	flow index in the Herschel-Bulkley model
39	SC, SCP	sponge cake, enriched in pulse protein, respectively
40	T	temperature
41	WC	Water content, expressed on a total wet basis
42	$\alpha_G, \alpha_{\tau_c}, \alpha_{\tau_y}, \alpha_K$	interaction coefficients of food with water based storage modulus, characteristic
43		stress, yield stress, consistency, respectively
44	γ, γ_c	strain and its value at intersection of G' and G'' curves
45	$\dot{\gamma}_{app}, \dot{\gamma}_w$	apparent and real wall shear rate
46	$\dot{\epsilon}$	deformation rate
47	$\eta_{app}, \eta^*, \eta, \eta_E$	apparent, complex, shear and elongational viscosity, respectively
48	ω	pulsation (oscillatory rheometry tests)
49	$\tau_w, \tau_c, \tau_s, \tau_{sc}$	wall shear, characteristic, yield (Hersche-Bulkley), corrected stress
50	τ_{c0}, τ_{s0}	dry bolus theoretical values of characteristic and yield stress, respectively

51

52

53 1. Introduction

54 Food Oral Processing (FOP) is a key step for food digestion. Its first aim is to form a food
55 bolus that can be swallowed safely (Chen, 2009 ; Stokes, Boehm & Baier, 2013). It is also the first
56 interaction of our body with food in the digestive system. During oral processing, food is reduced in
57 size and lubricated to form a bolus in preparation for swallowing and digestion. Simultaneously,
58 volatile chemicals from the food move to olfactory and taste receptors, food particles interact with
59 oral surfaces, and the net result is an evaluation of taste, aroma, and texture. The rheological
60 properties of the bolus are a link between food texture, its breakdown and its capacity to be
61 swallowed, and they are modified by the saliva uptake. Consequently, the knowledge of bolus
62 rheological properties is important to understand the dynamic changes in food structure that take
63 place during FOP (Morell, Hernando & Fiszman, 2014). Consequently, there is a need to develop
64 methods for assessing food breakdown during chewing and interaction with saliva (Boehm, Warren,
65 Baier, Gidley & Stokes, 2019).

66 The food bolus experiences a large range of shear rate and also extensional flow during oral
67 processing. From apparent viscosity (η_{app}) measurements, a model was built to represent the bolus
68 breakdown of cereal foods, such as sponge cake and brioche, during chewing (Assad-Bustillos,
69 Tournier, Septier, Della Valle & Feron, 2019a). This model allowed to derive a coefficient relating
70 bolus viscosity to its water content, which was defined as a coefficient of interaction « α » between
71 saliva and food (Assad-Bustillos et al., 2020). The variations of α underlined the influence of protein
72 enrichment on the oral processing of these cereal foods. It also showed that the study of FOP is an
73 essential step in food design, in the case of enrichment of foods by legume proteins. Moreover, a
74 correlation between η_{app} with oral comfort for low fat cereal foods has been established, which just
75 confirmed how important are the bolus shear and extensional viscosities for the ease of swallowing
76 (Marconati et al., 2019).

77 Saliva contains water at 99%, plus other components, such as mucin, and its properties have a
78 large variability depending on individual and stimulation conditions (Haward, Odell, Berry & Hall,
79 2011; Mosca & Chen, 2017). So the increase of bolus water content (WC), due to saliva flow during
80 chewing, is a common important feature in FOP. This is especially true for cereal products which
81 contain a large amount of amorphous starch, knowing the role of water as a plasticizer for
82 hydrophilic food components, such as amorphous starch. So, there is an interest to study the WC
83 dependence of bolus rheological properties of cereal food boluses.

84 Surprisingly, there are quite few studies dealing with the rheological properties of food bolus.
85 This can be due (1) to the difficulty of performing rheological measurements on real boluses, and (2)
86 to the uncertainty about the relevant rheological property for food oral processing. To overcome the

87 former difficulty, artificial boluses can be considered, provided that they are representative of real
88 ones. By doing so, it is possible to address the latter difficulty by performing different rheological
89 tests under a wide range of strain and strain rate conditions.

90 Given this context, the aim of this work is to determine the rheological properties of artificial
91 boluses of cereal foods in order to derive coefficients that help to quantify the interactions of foods
92 with saliva. For this purpose, artificial boluses are prepared under conditions as close as possible to
93 those encountered in FOP, to avoid physiological interindividual variability and to focus on bolus
94 rheology and the influence of water content. Bolus viscoelastic properties are investigated in the
95 linear and non-linear viscoelastic domains, using oscillatory shear rheometry, and flow properties are
96 measured by capillary rheometry. In addition to insights on food bolus structure, the variations of the
97 rheological properties with WC are determined for two types of cereal foods: a soft food with
98 intermediate moisture and a brittle dry one, as well as their corresponding version enriched in plant
99 protein.

100

101

102 **2. Material and methods**

103 ***2.1. Cereal foods and bolus preparation***

104 Four cereal food products were studied: two soft foods (sponge cake, SC) and two brittle
105 ones (extruded, E). One SC had a standard formulation (SC) and the other one was enriched with pea
106 proteins and held the claim “high in protein” (SCP). Both were provided by CERELAB® (Aiseray,
107 France). One extruded food is a commercial flat bread (EF, Les craquantes EPI d’OR™) and the other
108 one is made by extrusion of pea flour (EFP), as described in detail by Kristiawan et al. (2018). Their
109 composition, moisture content and density are reported in Table 1. Besides various differences,
110 especially starch content, the difference of water content makes the food soft (SC) or brittle (E).

111 In order to prepare artificial boluses, foods were fragmented and impregnated with water,
112 the main component (99%) of human saliva. This study focuses on the role of water, because the
113 addition of mucin and salts has been precedingly shown not to modify the rheological properties of
114 sponge cake boluses (Gibouin, Della Valle & van der Sman, 2019 a,b). In addition, the role of α -
115 amylase on rheological properties is discarded, in a first approach. The role of real saliva, and
116 especially of α -amylase will be discussed when comparing our results with those obtained for real
117 boluses, in section 3.3. Water was added at different levels, in order to obtain a bolus, homogeneous
118 at bare eye, and to cover the range of water content of food bolus during chewing, in agreement
119 with values found in literature, up to 60% for sponge cake and 80% extruded foods, in total wet
120 content (Assad-Bustillos et al., 2019a; Loret et al., 2011).

121 Before water addition, sponge cakes and extruded foods were fragmented with a commercial
122 blender(MagiMix, France) or manually using a mortar, respectively, until a particle mean size of 1mm
123 is reached, as measured with a vibrating sieves (Reitsch, F95610 Eragny). This size value is chosen
124 close enough to the particle size in real boluses at the first step of chewing. It has also been checked
125 that the particle size distribution is in agreement with the distribution in real boluses (Assad-Bustillos
126 et al., 2019b), and that in the range [1, 10mm], the particle size did not affect significantly the
127 rheological properties (Gibouin et al., 2019 a,b).

128 **2.2. Viscoelastic properties and oscillatory shear measurements**

129 Viscoelastic properties of bolus were determined with a controlled strain rheometer (ARES,
130 TA Instruments), provided with a plate-plate circular geometry: diameter = 4.0cm and gap = 2.5mm.
131 The temperature is controlled with a Peltier device and set to 23°C. The bolus sample is placed on the
132 lower plate and is gently squeezed to ensure surface contact. The variations of storage (G') and loss
133 (G'') moduli, with strain were determined at three different frequencies: $\omega = 10\text{rad/s}$, $\omega = 1\text{rad/s}$
134 and $\omega = 0.1\text{rad/s}$. The imposed strains ranged from 0.01% to 400% according to a logarithmic
135 distribution and with 10 points per decade. Each measurement is duplicated and the sample is
136 removed and replaced before each test. Moduli and complex viscosity η^* were determined in the
137 linear viscoelastic regime (imposed strain $\gamma = 0.5\%$) by applying a frequency sweep from 0.1rad/s to
138 100rad/s. The frequency distributions are also logarithmic with 10 points per decade and the
139 measurements are duplicated. All these measurements were achieved on bolus with various water
140 contents WC from 0.3 to 0.57 kg water / kg bolus on total wb (SC, SCP) and 0.68 to 0.8 kg water / kg
141 bolus on total wb (EF, EFP), in total wet basis.

142 **2.3. Flow properties and capillary rheometry measurements**

143 Flow properties are determined with a capillary rheometer with pre-shearing, Rheoplast, that
144 has been applied and described in detail by Della Valle, Vergnes & Lourdin (2007) and Nunez, Della
145 Valle & Sandoval (2010), who determined the viscous properties of starchy materials and cereal
146 foods, respectively, under extrusion conditions. In the following, we will only describe its main
147 working steps. In the case of food bolus, we did not use the pre-shearing function, because the
148 fragmentation has already been performed when preparing bolus with the blender.

149 All the tests are made at room temperature ($T = 23^\circ\text{C}$). The measuring chamber before the
150 capillary die is fed with the bolus by the vertical motion of an annular piston at a constant speed of
151 1mm/s. Then, the injection piston (diameter $D_p = 16\text{mm}$) is moved vertically at a constant speed of
152 0.5mm/s to fill the capillary die. Three capillary dies (diameter $D = 1\text{mm}$, entry angle = 90°) are used
153 with different die ratios L/D (32, 16 and 8). After a 15 s relaxation time, pressure is measured for
154 different decreasing speeds of the injection piston, each speed step for a time interval of about 15s,

155 ranging from 2 mm/s to 0.002mm/s, which leads to apparent shear rate values $3000 \geq \dot{\gamma}_{app} \geq 3 \text{ s}^{-1}$.
156 At the end of this sequence (about 2 mn), pressure measurement is repeated at the two largest
157 speed values, in order to check sample stability, and a pressure profile $P(\dot{\gamma}_{app})$ is obtained.

158 This procedure has been applied to every sample for the same range of water content values
159 as for oscillatory shear measurements (2.2). 15 to 20g of bolus are needed to obtain a single pressure
160 profile. Data treatment is performed according to usual procedure for capillary rheometry as
161 described in detail by Della Valle et al. (2007) and Nunez et al. (2010). The wall stress τ_w is derived
162 from pressure measurements, using Poiseuille law, after application of Bagley's corrections. The flow
163 index n is determined and the real value of the shear rate $\dot{\gamma}_w$ is calculated after Rabinowitsch
164 analysis. Finally, the shear viscosity η is defined as the ratio $\tau_w/\dot{\gamma}_w$. Using entrance effects from
165 Bagley correction, the elongational viscosity η_E and the deformation rate $\dot{\epsilon}$ may also be derived,
166 according to the Cogswell's method developed for melts polymers (Cogswell, 1972).

167 Flow curves (τ_w or $\eta(\dot{\gamma}_w)$) obtained for different moisture contents were fitted according to
168 appropriate rheological model and then shifted (translated) into a master curve to determine the
169 model parameters. This procedure, based on the time-temperature superposition principle, for the
170 rheological properties of polymers, has been already adapted by Della Valle et al. (2007) to the time-
171 plasticizer content superposition, in the case of plasticized starches. In this study, the shifting factors
172 were derived using Python (Python Software Foundation) according to the procedure developed by
173 Saboo *et al.* (2018).

174 **2.4 Imaging**

175 Fragmented boluses of sponge cakes and extruded foods were prepared in the same way as
176 for rheological measurements and water was added to obtain the necessary dilution before inserting
177 between glass blades, and observed on a binocular stereomicroscope Leica with retro-lighting ($\times 35$;
178 Leica Microsystems, Conrad Electronics, France). No specific staining was used.

179

180

181 **3. Results and discussion**

182 **3.1. Viscoelastic properties**

183 Within the linear domain ($\gamma < 1\%$), harmonic measurements performed at small strain
184 amplitude, led to similar bolus mechanical spectra ($G'(\omega)$, $G''(\omega)$) whatever the food considered and
185 its water content (Fig.1) : G' and G'' were slightly increasing functions of pulsation (or frequency) and
186 all bolus exhibited a storage modulus larger than the dissipative one ($G' > G''$) in the range of
187 frequency tested, and $\tan \delta$ remained nearly constant (≈ 0.2). Clearly boluses behave more like solid
188 than fluids. Such spectra are usually typical of a viscoelastic network, with the frequency window of

189 the test framing a part of the viscoelastic plateau. However, in the case of these artificial bolus, no
190 structural interpretation can be given for the entities involved in such a network, at this stage. In
191 many cases, $G''(\omega)$ curves exhibited a shallow minimum within the frequency interval ($0.1 < \omega < 1$
192 rd/s). The frequency and the G' value corresponding to this G'' minimum can be taken conventionally
193 as representative of the characteristics (frequency and modulus) of the viscoelastic plateau
194 (Ferry,1980). However, the frequency of the minimum depended on the bolus, and in some cases, it
195 was not really observed. Therefore, for all our samples, we took the G' value at 1 rad/s as an
196 empirical measure of the viscoelastic plateau modulus. Fig.1 also showed that, for all food boluses, a
197 regular decrease of both moduli was observed as water content increased, which, as expected,
198 indicated that water acts as a lubricant. It also suggested that, for SC bolus, the enrichment in protein
199 slightly increased the values of moduli, and reduced its sensitivity to water content. Conversely, pea
200 based extruded snacks (EFP) led to boli with much larger moduli, about 10 times, than extruded flat
201 bread (EF), but displayed similar water sensitivity.

202 The values of storage modulus at viscoelastic plateau $G'(\omega \leq 1 \text{ rd/s})$ were negatively
203 correlated to the water content (Fig.2). These variations can be described by the equation :

$$204 \quad G' = G'_0 * \exp [- \alpha_G * WC] \quad (1)$$

205 G'_0 represents the theoretical value of storage modulus for dry bolus ; parameter α_G . reflects
206 the interaction of the food with water and can be envisioned as a water plasticization coefficient. The
207 values of these parameters are reported in Table 2. Similar results could have been obtained by
208 shifting and superimposing G' (and G'') curves for a given moisture content as performed by van der
209 Sman and Mauer (2019), in the case of starch/sugar/polyol mixtures, and by Costanzo et al. (2019)
210 for gluten / water / ethanol blends. Besides extending the time-temperature superimposition
211 principle to time-solvent in the case of biopolymers, these works underlined the importance of
212 intermolecular interactions, mainly H bonds. Such interactions could be captured by the ratio of
213 sample temperature to glass transition temperature of the biopolymer, which is a function of its
214 solvent content. Regarding food boluses, our results suggest that the protein enriched sponge cake
215 (SCP) interacts the least with water, likely because of the hydrophobic nature of added pea isolates,
216 whereas globulins interactions with glutenins might also be inferred for the decrease of water
217 sensitivity (Lambrecht, Deleu, Rombouts & Delcour, 2018). Conversely, extruded pea flour (EFP)
218 shows larger interaction with water than flat bread (EF), likely because hemicellulosic compounds,
219 contained in pea flour, have a strong water retention capacity that largely balances the hydrophobic
220 influence of pea isolates observed for SCP (Kristiawan et al., 2018).

221 For all moisture contents and foods, the variations of G' and G'' moduli with the applied
222 strain γ exhibited the same patterns (Fig. 3). From this graph, three main zones may be delineated:

223 first the linear viscoelastic regime ($\gamma \leq 1\%$), where moduli are constant, with $G' > G''$ like for a gel,
 224 then, a transient regime, where storage modulus decreases and crosses G'' curve, which can be
 225 considered as plastic region, and, finally, a non-linear regime where both moduli decrease, with $G'' >$
 226 G' , indicating that bolus starts to flow. This behaviour is typical of the loss of structure and of the
 227 flow of the material under increased strain. Since it holds for all bolus samples, we can define the
 228 stress τ_c , at the crossing of G' and G'' as a characteristic parameter of this behaviour:

$$229 \quad \tau_c = \gamma_c * G^* \quad (2)$$

230 G^* being the value of the complex modulus and γ_c the strain value at intersection of G' and
 231 G'' curves ($G'=G''$). Another characteristic stress maybe defined, by the value obtained at the end of
 232 the linear viscoelastic domain, defined by the crossing of the horizontal tangent of G' in the linear
 233 domain with the tangent to G' curve during plastic flow (see Fig.3). It is found that these values are
 234 highly correlated to the values of τ_c ($r^2 > 0.9$, see Appendix 1), so, in the following, τ_c is considered to
 235 characterise the transition of bolus to flow. The values of τ_c are negatively correlated to the water
 236 content (Fig.4). These variations can be described by the equation :

$$237 \quad \tau_c = \tau_{c0} * \exp [- \alpha_{\tau_c} * WC] \quad (3)$$

238 τ_{c0} is the theoretical value of characteristic stress for the dry bolus; parameter α_{τ_c} reflects the
 239 interaction of the food with water, like a water plasticization coefficient. The values of these
 240 parameters are reported in Table 2. At first glance, they confirm the trends observed in the linear
 241 viscoelastic domain, when considering α_G values : protein enriched sponge cake (SCP) interacts the
 242 least with water, again due to the hydrophobicity of pea isolates, whereas extruded pea flour (EFP)
 243 shows larger interaction with water than flat bread (EF), which, again, may be attributed to the
 244 presence of hemicellulosic compounds in pea flour. However, for extruded products, the values of
 245 α_{τ_c} are larger than those of sponge cakes, and the variations of characteristic stress obtained for EF
 246 and EFP are close to each other (Fig.4). This result indicates that the stress needed to make the bolus
 247 flow is more influenced by water for extruded cereal foods, than for sponge cakes, whether they are
 248 enriched in plant proteins or not. Moreover, the huge value of initial stress τ_{c0} , found for extruded
 249 products (Table 2, $\tau_{c0} > 100$ MPa), confirms that, overall, large amounts of water ($WC \geq 60\%$) are
 250 needed to elaborate a flowable bolus from these foods that contain a large amount of hydrophilic
 251 compounds like amorphous starch.

252 **3.2 Flow properties**

253 From the pressure profiles $P(\dot{\gamma}_{app})$ obtained for different capillary geometries (L/D ratio),
 254 and using Poiseuille relation, flow curves can be derived, representing the variations of the wall shear
 255

256 stress τ_w as a function of apparent shear rate or $\tau_w (\dot{\gamma}_{app})$ for food boluses at different amount of
 257 water WC (Fig.5). As expected, the larger WC, the lower the apparent viscosity, defined by the ratio
 258 $\tau_w/\dot{\gamma}_{app}$: flow curves show that viscosity decreases by a factor of 10 when WC is increased by 0.10
 259 for SC foods, whereas the decrease is lower for extruded foods. Some curves display a dispersion of
 260 experimental points, especially at larger moisture content. Indeed, in these conditions, flow becomes
 261 less steady and measurement accuracy lower, given the low level of pressure reached in the
 262 capillary, and also possible slip-stick phenomena. However, all curves show a similar increasing trend,
 263 and some of them suggest the existence of a yield stress at lower shear rate (like for SC at WC= 0.28
 264 and 0.36, for instance). Therefore, after having converted apparent shear rate values $\dot{\gamma}_{app}$ into wall
 265 shear rate $\dot{\gamma}_w$, using Rabinowitsch correction, all curves are fitted using the Herschel-Bulkley model,:

$$266 \quad \tau_w = \tau_s + K * \dot{\gamma}_w^n \quad (4)$$

267 where τ_s is the yield stress, K the consistency (Pa.sⁿ), and n the flow index.

268 Although fitting is acceptable ($r^2 > 0.75$), considering the dispersion mentioned before, it is thought
 269 that determining coefficients τ_s , K and n for each WC value could increase the uncertainty. Moreover,
 270 the flow index does not change significantly for each product, whatever the value of WC. Therefore,
 271 for each product, a master curve is determined by adapting the time-temperature principle, to
 272 superpose flow curves, obtained from bolus at different water content. Hence, each flow curve is
 273 shifted to a reference curve, at a given WC value, by plotting the reduced shear stress (τ_w / a) as
 274 function of reduced shear rate ($\dot{\gamma}_w * a$), a being the shift factor. This procedure is illustrated in
 275 Appendix 2. The Herschel-Bulkley coefficients of the reference curve are recalled in Table 3, for each
 276 product. The values of the shift factor a vary between 0.016 and 27.8 and they are directly correlated
 277 to the water content, all food products being considered together (Fig.6a). In a first approach, this
 278 correlation suggests that the influence of water on the viscous behavior of the bolus in shear flow is
 279 similar for the four different cereal foods. Secondly, by applying (eq.4) to $(\tau_w/a) [a*\dot{\gamma}_w]$, this
 280 correlation can be used to calculate, for any WC value, the corrected values for the coefficients of the
 281 Herschel Bulkley model by :

$$282 \quad \tau_{sc} = \tau_s / a(WC) \quad \text{and} \quad K_c = K / [a(WC)]^{n+1} \quad (5)$$

283 The numerical values of τ_{sc} , K_c and n , for all values of WC and products tested, are reported
 284 in Appendix 3. Note that the value of flow index n did not vary with WC. Furthermore, using
 285 correlation from Fig.6a and eq. (5), flow curves for the boluses of the four products can be derived
 286 for any WC value. For instance, for WC=0.6, taken as a typical value in the interval [0.28, 0,8], flow
 287 curves representing the shear viscosity η as a function of shifted shear rate ($\dot{\gamma}_w * a$) can be drawn
 288 (Fig.6b). These curves show that for low shear rate values, the viscosity of the bolus is very close to
 289 each other, whereas for larger values ($\dot{\gamma}_w * a > 10s^{-1}$), the two extruded products (EF and EFP) lead to

290 much larger viscosity than sponge cakes, whether they are enriched in plant protein or not. The
291 increase of slope, observed at lower shear rate values, underlines the presence of the yield stress,
292 and it is enhanced for SC and EFP. In line with the preceding results obtained for the viscoelastic
293 properties, the variations of the Herschel-Bulkley coefficients τ_{sc} and K_c with WC can be represented
294 (Fig.7) and fitted by the following relations :

$$295 \quad \tau_{sc} = \tau_{s0} \cdot \exp [-\alpha_{\tau} * WC] \quad \text{and} \quad K_c = K_{c0} \cdot \exp [-\alpha_K * WC] \quad (6)$$

296 from which the values of τ_{s0} , α_{τ} , K_{c0} and α_K are extracted and reported in Table 2. In
297 addition, variations of consistency with water are very close to each other for the four products (Fig.
298 7b), and a common trend can be found for K_c variations, giving a mean value for $\alpha_K = 10.25$ ($r^2 = 0.9$).
299 Regarding α_{τ} and α_K variations, the trends obtained here are different from those observed for the
300 viscoelastic properties since standard products (SC and EF) display the lower α_{τ} and α_K values.
301 Moreover, α_{τ} and α_K values are correlated. These results show that, during the flow, the products
302 enriched with plant proteins interact more with water than their standard counterpart. In other
303 words, the presence of proteins increase the bolus flow sensitivity to water, which suggests that flow
304 could contribute to bolus destructuring by disrupting food particles or releasing protein aggregates.

305 The same procedure can be applied to determine the apparent elongational viscosity of
306 boluses, by taking into account entrance pressure effects from capillary rheometry tests. Then, using
307 the same time-water superposition principle, master curves can be determined, for instance at WC
308 =0.6 (see Appendix 4). Indeed, very little differences can be observed between the four foods.

309

310 **3.3 Bolus structure and rheological properties relationships**

311 First, the values found for coefficients α were in the same numerical interval [5, 31],
312 regardless the rheological property. These values are in the same interval as the values of coefficients
313 of starch plasticization by water, found for starchy materials and cereal foods under extrusion
314 conditions (Della Valle et al., 2007; Nunez et al., 2010). Clearly, this result suggests that starch /water
315 interactions have a significant role in the rheological behavior of the bolus and its breakdown during
316 FOP. However, these values stand for starch melts as encountered during extrusion, i.e. at high
317 temperature and shear, where starch granules are broken and polymers released. Food boluses can
318 hardly be compared to starch melts. By the way, Cox-Merz rule does not apply, unlike polymer
319 melts, since complex viscosity always took values larger than those of steady shear viscosity (as
320 illustrated in Appendix 5), which reflects that the structure of bolus changed during steady flow.

321 Moreover, boluses are made of particles, of typical size 1mm, which are not expected to
322 fragment during flow, but rather to deform, as shown by the micrographs of diluted boluses (Fig.8).
323 Sponge cake (SC) bolus presents a rather uniform appearance of a cohesive mass of blurred

324 aggregated particles, whereas enriched protein sponge cake (SCP) is more heterogenous, with darker
325 parts and bigger entities (> 1 mm), separated by water. Extruded flat bread bolus (EF) also presents a
326 cohesive morphology, whereas extruded pea flour bolus (EFP) presents a clear picture of
327 agglomerated and elongated particles (length > 1 mm, width < 1 mm). These images suggest that the
328 foods are not destructured in the same way after fragmentation and hydration. So it is not surprising
329 that their characteristic rheological properties are not fully correlated.

330 In spite of these visual differences, they may be all envisioned as concentrated suspensions of
331 deformable particles (Fig.9). At lower strain the suspension is jammed, because of particles swelling
332 due to water absorption (Fig.9b), which gives the bolus a solid-like behavior, in the viscoelastic
333 domain. At larger strain, hence larger stress ($\tau > \tau_c$ or τ_s), the suspension may still be partially
334 jammed, because, in the case of standard foods, hydrophilic particles still swell (Fig.9c). Conversely,
335 the particles of protein enriched foods, being less hydrophilic, swell less, water acts as a lubricant
336 which favors bolus flow (Fig. 9d). This interpretation would explain why the values of coefficient α
337 referring to flow properties (yield stress τ_s and consistency K) are larger for the protein enriched
338 foods than for their standard counterpart. More experiments, for instance using measurements of
339 water absorption or swelling index on such products, and even comparison with settling ratio
340 (Boehm et al. 2019) could contribute to test this hypothesis. Whether this transition occurs at the
341 value of characteristic stress τ_c or yield stress τ_s is still to be determined precisely, although both
342 properties are correlated (Fig.10). The question is significant since both properties might be relied on
343 for the control of swallowing.

344 Clearly, before extending these rheological measurements to assess the interactions of saliva
345 with food, it is necessary to test the influence of other saliva components on bolus rheological
346 properties. Recently, these properties were measured on bolus made by mixing same foods (sponge
347 cake) with artificial saliva, containing salt and mucin, and no significant difference was detected
348 when compared with bolus made with water (Gibouin et al., 2019b). The influence of the addition of
349 α -amylase, another component of saliva, on bolus rheological properties is still questionable. There is
350 a general agreement that salivary α -amylase plays an important part in destructuring cereal foods,
351 like bread, during the gastric phase (Bonhorst & Singh, 2013; Pentikäinen et al., 2014; Freitas,
352 Feunteun, Panouille & Souchon, 2018). But the short residence time of the food in the mouth may
353 explain the little influence of α -amylase on bread destructuring during FOP, assessed by viscosity
354 measurements (Le Bleis, Chaunier, Montigaud & Della Valle, 2016).

355 Regarding FOP, another point that confirms the relevance of our measurements comes from
356 some results obtained when characterizing real boluses. Results obtained by Loret et al. (2011)
357 measuring yield stress on cereal flakes boluses collected before swallowing for 11 subjects, hence for

358 different saliva contents, lead to a value of α of about 8, i.e. in the interval found in this study. For
359 sponge cake boluses, the values of coefficient α found for apparent viscosity were also in the same
360 interval (17 and 11 for standard and protein enriched sponge cake, respectively) (Assad-Bustillos et
361 al., 2020). Furthermore, they ordered in the same way as the values of α_{τ_c} found in the present
362 study (9.3 and 4.8, see Table 2). This result suggests that the coefficient α_{τ_c} contributes to assess
363 food-saliva interaction and that characteristic stress τ_c is the property that matters to define bolus
364 destructuring. Although more work is necessary to ascertain this trend, it is possible, and rather
365 simple, to extend these rheological methods to other foods. In turn, this would help to design and
366 test foods that would have a specific behavior during chewing.

367

368

369 **4. Conclusion**

370 Our results show that the rheological properties of artificial food cereal boluses can be
371 determined in a wide range of strain and strain rates, using different methods, in the range of water
372 content encountered during FOP. For the four foods tested, hydrated boluses exhibited same
373 behavior. First, at low strain, in the linear viscoelastic domain, bolus had a gel like behavior
374 characterized by the viscoelastic modulus G^* . Then, destructuring occurs at larger strain ($\gamma \geq 0.1$),
375 where a characteristic stress τ_c can be delineated from the intersection between curves of storage
376 and dissipative moduli. During steady flow, bolus behavior was found to follow Herschel-Bulkley
377 model from which yield stress τ_s and consistency K were derived; master curves could be determined
378 to compare the viscous behavior of the four products. At larger shear rate ($\dot{\gamma}_w \geq 10 \text{ s}^{-1}$), viscosity was
379 found larger for extruded foods without any effect of protein content. The variations of these four
380 rheological properties (G^* , τ_c , τ_s and K) with water followed an exponential decay, from which it was
381 possible to derive coefficients of interaction with water, for each property and product. Their
382 changes with product composition and structure were interpreted by envisioning the bolus as a
383 suspension of soft particles. The comparison of their values with those obtained for real boluses, and
384 their variations with protein content, suggest that rheological measurements are helpful to
385 characterize the interaction of food with saliva.

386

387

388 **Acknowledgements**

389 This work was carried out with the financial support of the regional programme "Food for Tomorrow
390 / Cap Aliment", which is supported by the French Region Pays de la Loire and the European Regional

391 Development Fund (FEDER). Florence' stay at UPV received the support of COST Action (CA15118 -
392 Mathematical and Computer Science Methods for Food Science and Industry).
393
394
395

396 **References**

- 397 Assad-Bustillos, M., Tournier, C., Septier, C., Della Valle, G., Feron, G. (2019a). Relationships of oral
398 comfort perception and bolus properties in the elderly with salivary flow rate and oral health
399 status for two soft cereal foods. *Food Research International*, 118, 13–21.
- 400 Assad-Bustillos, M., Tournier, C., Feron, G., Guessasma, S., Reguerre, A. L., Della Valle, G. (2019b).
401 Fragmentation of two soft cereal products during oral processing in the elderly: Impact of
402 product properties and oral health status. *Food Hydrocolloids*, 91, 153–165.
- 403 Assad-Bustillos, M., Tournier, C., Palier, J., Septier, C., Feron, G., Della Valle, G. (2020). Oral
404 processing and comfort perception of soft cereal foods fortified with pulse proteins in the
405 elderly with different oral health status. *Food & Function*, 11, 4535–4547.
- 406 Boehm, M.W., Warren, F.J., Baier, S.K., Gidley, M.J., Stokes, J.R. (2019). A method for developing
407 structure-rheology relationships in comminuted plant-based food and non-ideal soft particle
408 suspensions. *Food Hydrocolloids*, 96, 475–480.
- 409 Bonhorst, G.M., & Singh, P. (2013). Kinetics of *in Vitro* Bread Bolus Digestion with Varying Oral
410 and Gastric Digestion Parameters. *Food Biophysics* 8, 50–59
- 411 Chen, J. (2009). Food oral processing. A review. *Food Hydrocolloids* 23, 1-25.
- 412 Cogswell, F. N. (1972). Converging flow of polymer melts in extrusion dies. *Polymer Engineering &*
413 *Science*, 12, 64-73.
- 414 Costanzo S., Banc A., Louhichi A., Chauveau E., Wu BH., Morel MH., Ramos, L. (2020). Tailoring the
415 Viscoelasticity of Polymer Gels of Gluten Proteins through Solvent Quality. *Macromolecules*
416 53, 9470-9479.
- 417 Della Valle, G., Vergnes, V., and Lourdin, D. (2007). Viscous properties of thermoplastic starches from
418 different botanical origin. *International Polymer Processing*, 22, 471-479. Ferry, J.D. (1980).
419 Viscoelastic Properties of Polymers. Wiley, New York.
- 420 Freitas, D., Feunteun, S.L., Panouillé M., Souchon I. (2018). The important role of salivary α -amylase
421 in the gastric digestion of wheat bread starch. *Food & Function* 9, 200–208.
- 422 Gibouin, F., Della Valle, G. & van der Sman, R. (2019a). Mesures de viscosités de bols alimentaires
423 artificiels. *Rhéologie* 36, 15-20.
- 424 Gibouin, F., Della Valle, G. & van der Sman, R., (2019b). Viscosity of artificial chewed boluses of
425 cereal foods. *Edible Soft Matter 17th-19th April*, Le Mans, France.
- 426 Haward, S.J., Odell, J.A., Berry, M.A., Hall, T. (2011). Extensional rheology of human saliva. *Rheol*
427 *Acta*, 50, 869–879
- 428 Kristiawan, M., Micard, V., Maladira, P., Alchamieh, C., Maignret, J-E., Réguerre, A-L., Emin, A., Della
429 Valle, G. (2018). Multi-scale structural changes of starch and proteins during pea flour
430 extrusion. *Food Research International*, 108, 203–215.

431
432
433 Lambrecht, M.A., Deleu, L.J., Rombouts, I., Delcour, J.A. (2018). Heat-induced network formation
434 between proteins of different sources in model systems, wheat-based noodles and pound
435 cakes. *Food Hydrocolloids*, 79, 352-370
436 Le Bleis, F., Chaunier, L., Montigaud, P., Della Valle, G. (2016). Deconstruction mechanisms of bread
437 enriched with fibres during mastication. *Food Res. Int.*, 80, 1-11.
438 Loret, C., Walter, M., Pineau, N., Peyron, M. A., Hartmann, C., Martin, N. (2011). Physical and related
439 sensory properties of a swallowable bolus. *Physiology & Behavior*, 104, 855-864
440 Marconati, M., Engmann, J., Burbidge, A.S., Mathieu, V., Souchon, I., Ramaioli, M. (2019). A review of
441 the approaches to predict the ease of swallowing and postswallow residues. *Trends in Food*
442 *Science & Technology* 86, 281–297
443 Morell, P., Hernando, I., Fiszman, S.M. (2014). Understanding the relevance of in-mouth food
444 processing. A review of *in vitro* techniques. *Trends in Food Science & Technology* 35, 18-31
445 Mosca, A.C. & Chen, J. (2017). Food-saliva interactions: Mechanisms and implications. *Trends in Food*
446 *Science & Technology* 66, 125-134
447 Núñez, M., Della Valle, G., Sandoval, A. J. (2010). Shear and elongational viscosities of a complex
448 starchy formulation for extrusion cooking. *Food Res. Int.*, 43, 2093-2100.
449 Pentikäinen S, Sozer N, Närviäinen J, Ylätaalo S, Teppola P, Jurvelin J, Holopainen-Mantila U, Törrönen
450 R, Aura AM, Poutanen K. (2014) Effects of wheat and rye bread structure on mastication
451 process and bolus properties. *Food Res Int* 66:356–364
452 Saboo, N., Kumar, P. (2018). Equivalent slope method for construction of master curves. *Indian*
453 *Higways*, February, 19-28.
454 van der Sman R.G.M., Mauer L.J. (2019). Starch gelatinization temperature in sugar and polyol
455 solutions explained by hydrogen bond density. *Food Hydrocolloids*, 94, 371–380
456 Stokes, J.R. , Boehm, M.W., and Baier, S.K. (2013). Oral processing, texture and mouthfeel: From
457 rheology to tribology and beyond". *Current Opinion in Colloid & Interface Science* 18, 349-
458 359.
459
460

461 **List of figures**

462 Figure 1: Examples of mechanical spectra obtained for the artificial bolus in the linear viscoelastic
463 domain ($\gamma < 0.5\%$) for (a) standard sponge cake (SC), (b) sponge cake enriched with plant
464 proteins (SCP), (c) extruded flat bread (EF) and (d) extruded pea flour (EFP) for different
465 levels of water content WC as indicated in the graphs, on a total wet basis (the darker the
466 symbols, the larger the WC value).

467
468 Figure 2: Variation of storage modulus G' at viscoelastic plateau ($\omega = 1\text{rad/s}$) as function of the water
469 content of food bolus for SC (O, a), SCP (●, b), EF (□, c) and EFP (■, d). Straight lines feature
470 fitting by exponential functions ($r^2 > 0.96$) with parameters given in Table 2.

471
472 Figure 3: Example of strain sweep test result (here for SCS bolus, WC=0.57). Dotted vertical lines
473 delineate the three regimes of bolus behavior, viscoelastic, plastic and flow. The crossing
474 point ($G' = G''$) allows defining the characteristic stress τ_c .

475
476 Figure 4: Variation of characteristic stress τ_c at modulus crossing ($G' = G''$) as function of the water
477 content of food bolus for SC (O), SCP (●), EF (□) and EFP (■). Straight lines feature fitting by
478 exponential functions ($r^2 > 0.96$) with parameters given in Table 2.

479
480 Figure 5: Flow curves of cereal food boluses obtained by capillary rheometry, for three different
481 moisture contents WC (lowest O, medium ●, highest ●): SC (a), SCP (b), EF (c) and EFP (d).
482 Dotted lines are best fit by power law functions ($r^2 > 0.75$).

483
484 Figure 6: (a) Variations of the shift factor a applied to build a master curve from curves represented
485 in Fig.5, with water content WC for SC (O), SCP (●), EF (□) and EFP (■), dotted line showing
486 best fit $a = 8.10^{-4} \exp [12 \cdot WC]$ ($r^2 \approx 0.89$); and (b) flow curves derived from the Herschel-
487 Bulkley model applied for artificial bolus at WC=0.6, of sponge cake (black lines, SC and SCP)
488 and extruded bread (grey lines, EF and EFP), standard cereal foods (thin continuous, SC and
489 EF) and enriched in legume protein (dotted thick, SCP and EFP).

490
491 Figure 7: Variations of Herschel-Bulkley model's coefficients (defined in eq. (4) and (5)) with water
492 content of food bolus for SC (O), SCP (●), EF (□) and EFP (■): yield stress τ_{sc} (a) and
493 consistency K_c (b). Straight lines feature fitting by exponential functions ($r^2 > 0.96$) with

494 parameters given in Table 2, whereas thick dotted line (light grey) in (b) features the best fit
495 obtained by taking all boluses together into account ($K_c = 180 \exp [-10.25 * WC]$, $r^2=0.9$).

496

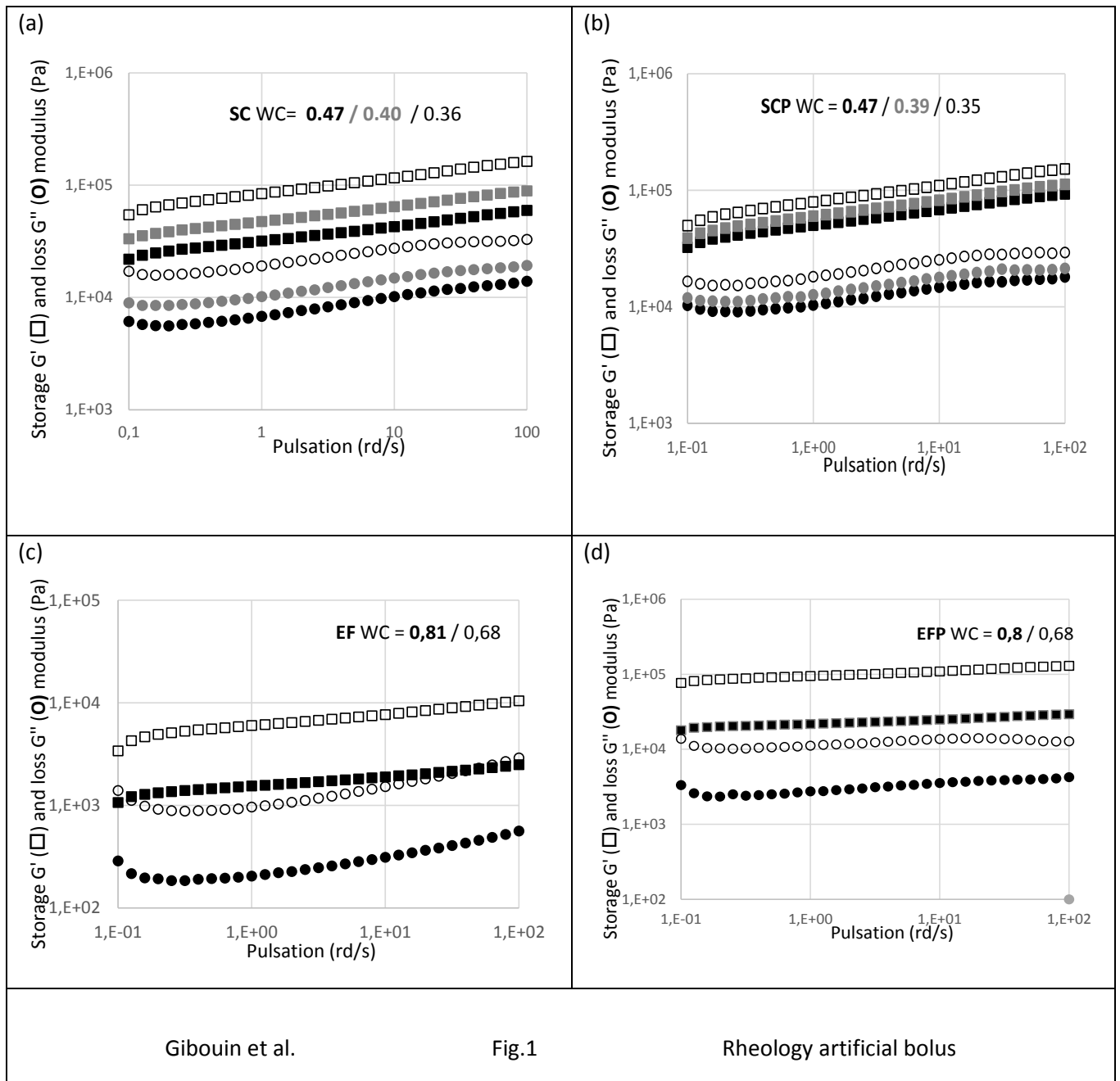
497 Figure 8: Micrographs of the artificial boluses of (a) standard sponge cake SC, (b) sponge cake
498 enriched with proteins (SCP, white stain on bottom left is water between food particles), (c)
499 extruded flat bread (EF) and (d) extruded pea flour EFP. Image width is 1cm. No specific
500 staining was used, so differences of shade (light / dark) reflect the matter concentration, i.e.
501 non-uniform thickness of the sample layer between blades, rather than specific composition
502 or structural state.

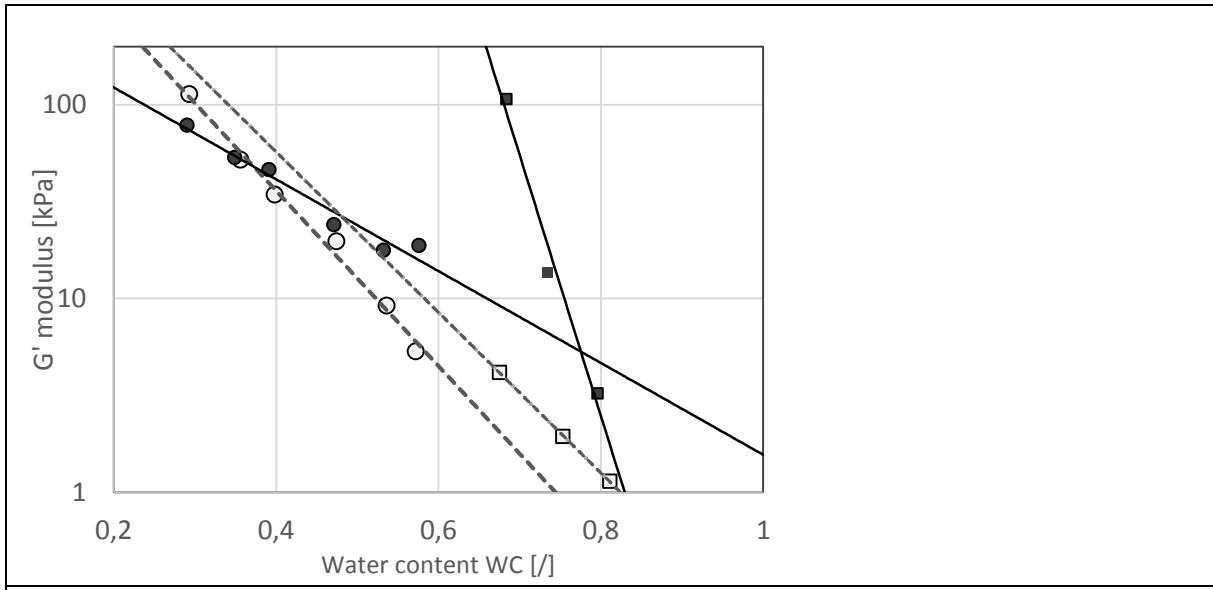
503

504 Figure 9: Schematic representation of bolus structure, envisioned as a suspension of more or less
505 swollen and deformable spherical particles: dry ground food (1mm) (a), wet particles in low
506 strain domain (or $\tau < \tau_s$ or τ_c) (b); destructured suspension of particles of standard (c) and
507 protein enrich foods (red spots symbolize proteic component (d)), at large strain ($\tau > \tau_s$ or τ_c
508).

509 Figure 10: Variations of the values of yield stress τ_s computed for the same WC as characteristic
510 stress τ_c for the boluses of the four cereal foods SC (O), SCP (●), EF (□) and EFP (■).

511



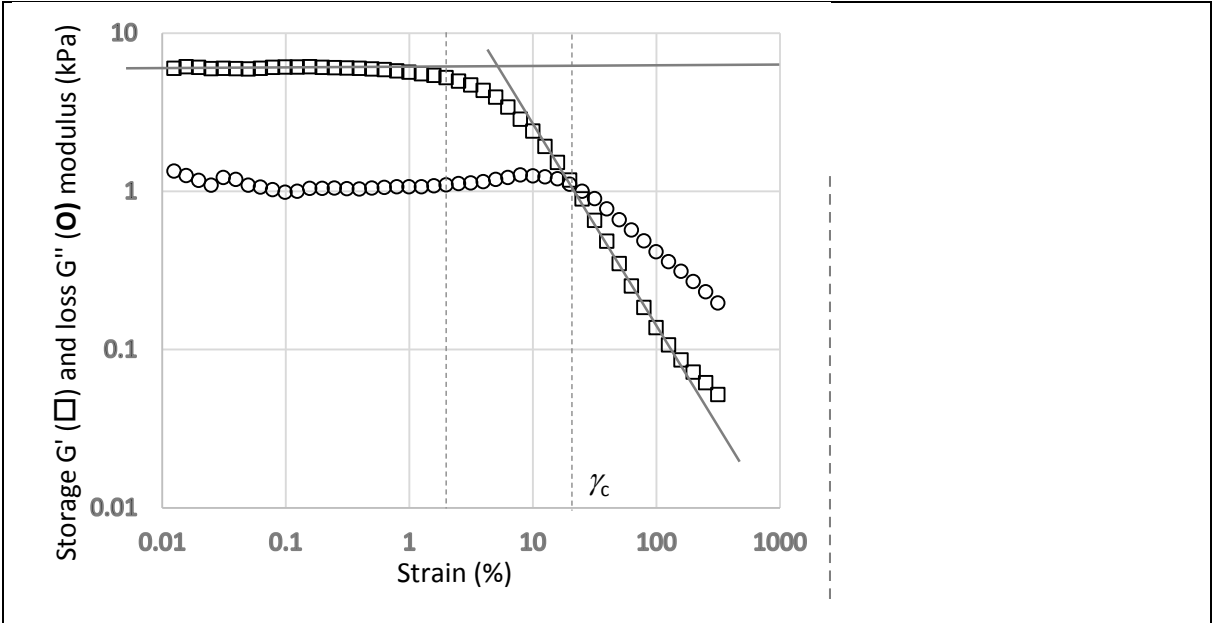


Gibouin et al.

Fig.2

Rheology artificial bolus

515



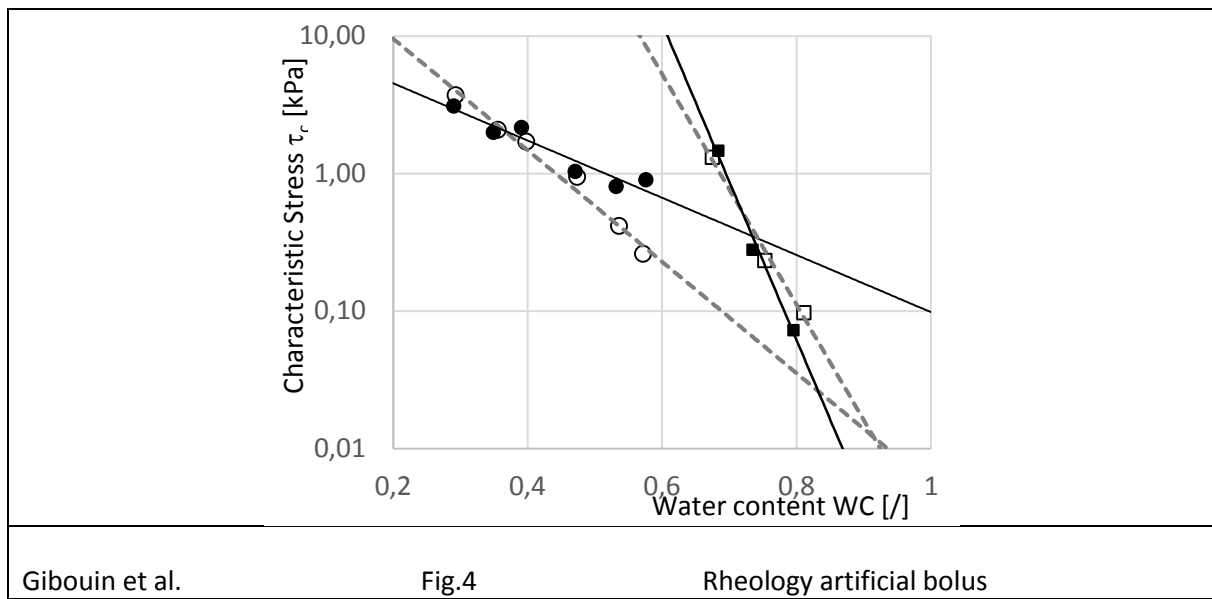
Gibouin et al.

Fig.3

Rheology artificial bolus

516

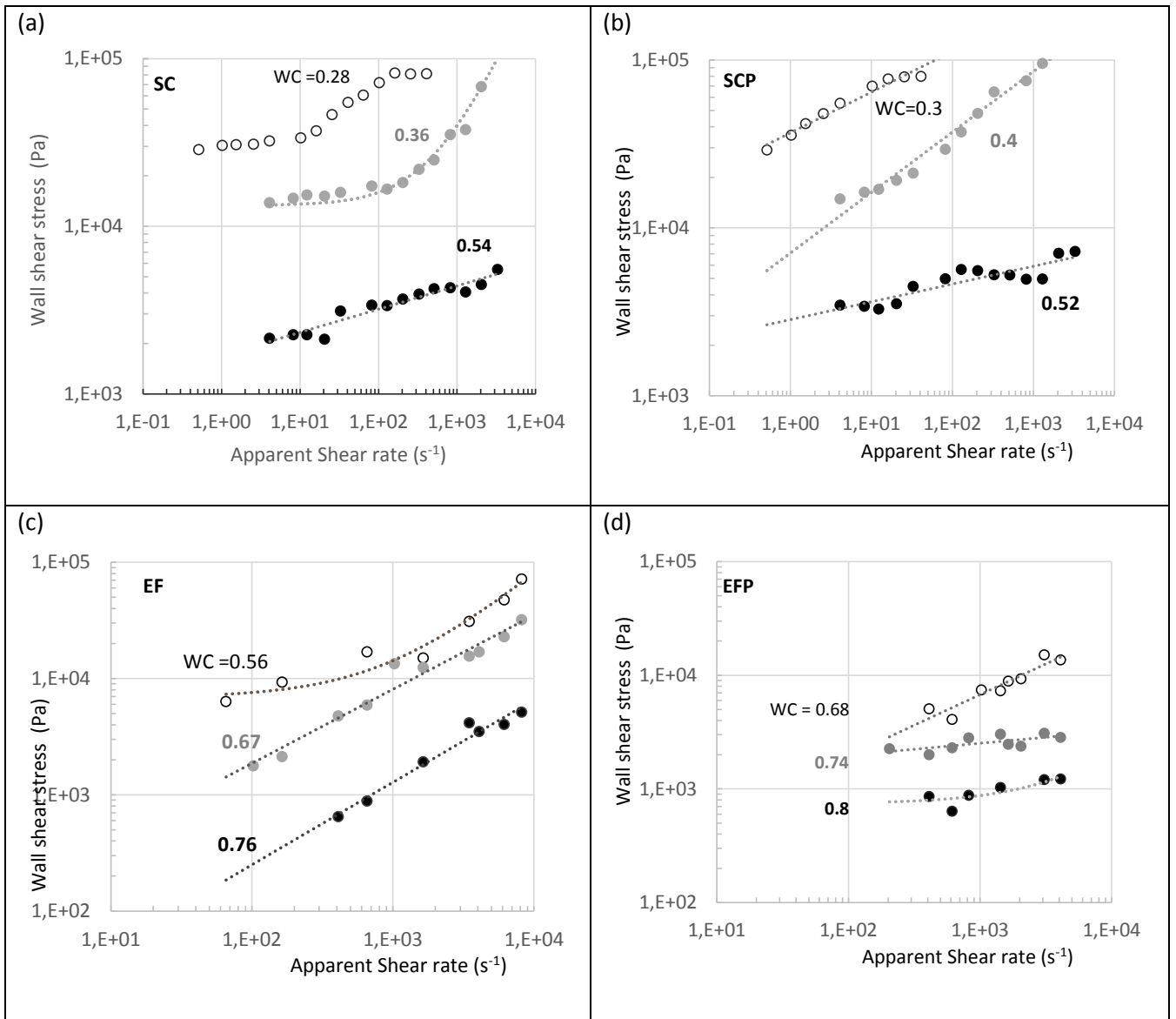
517



Gibouin et al.

Fig.4

Rheology artificial bolus



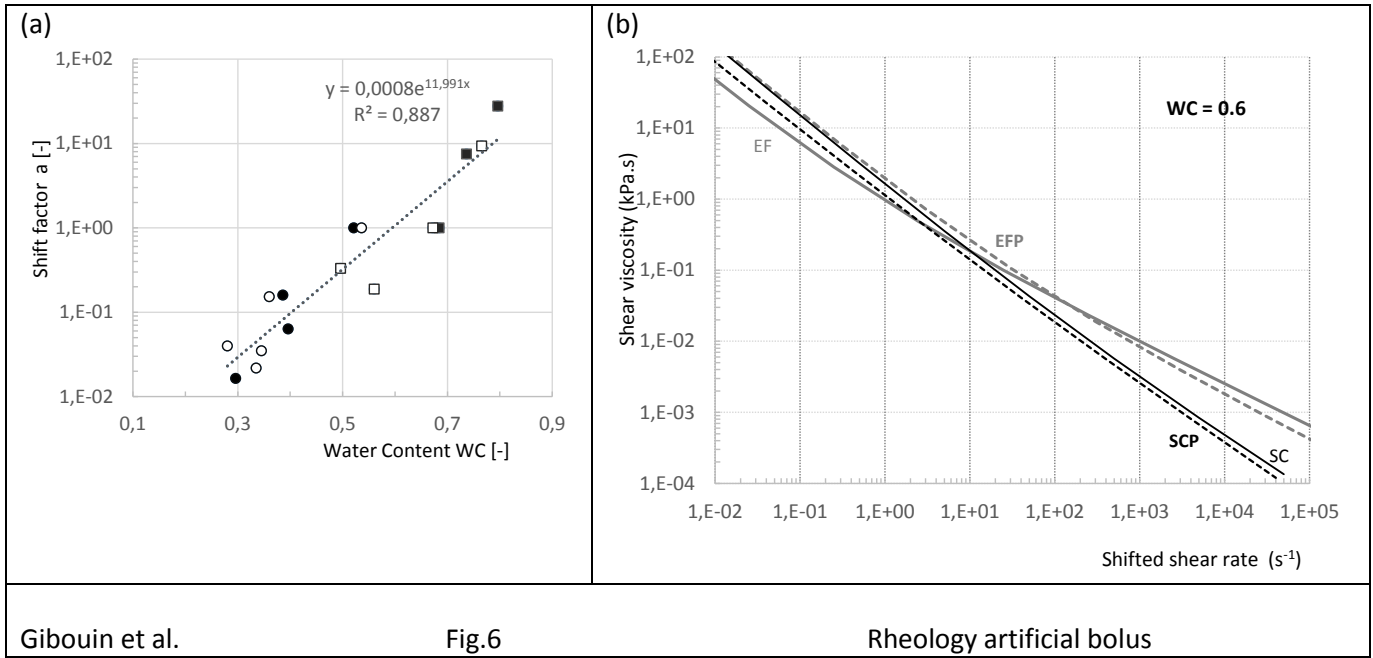
Gibouin et al.

Fig.5

Rheology artificial bolus

520

521



Gibouin et al.

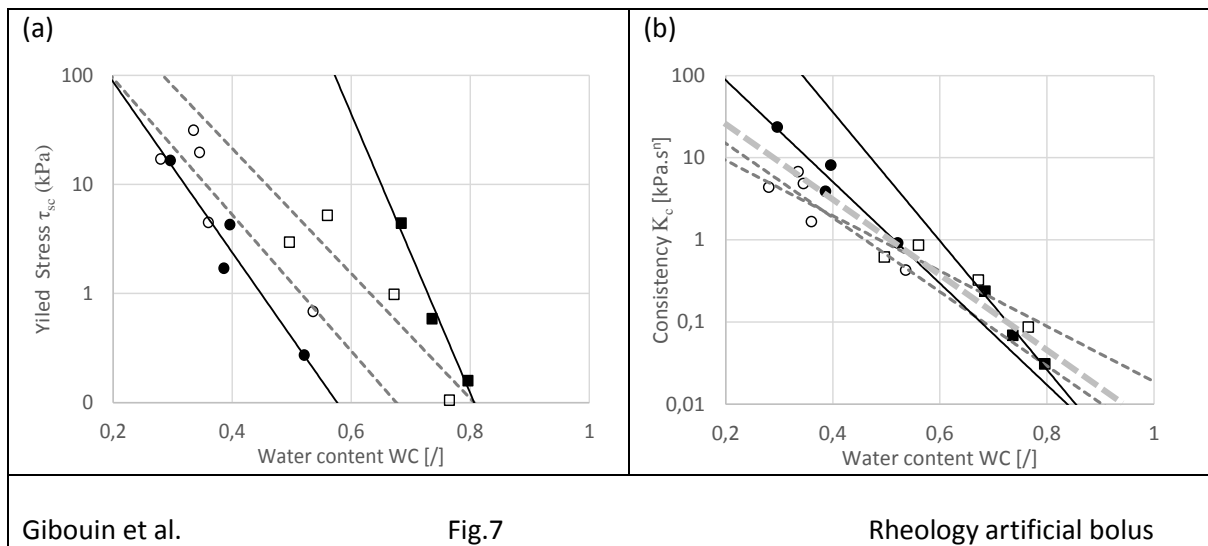
Fig.6

Rheology artificial bolus

522

523

524

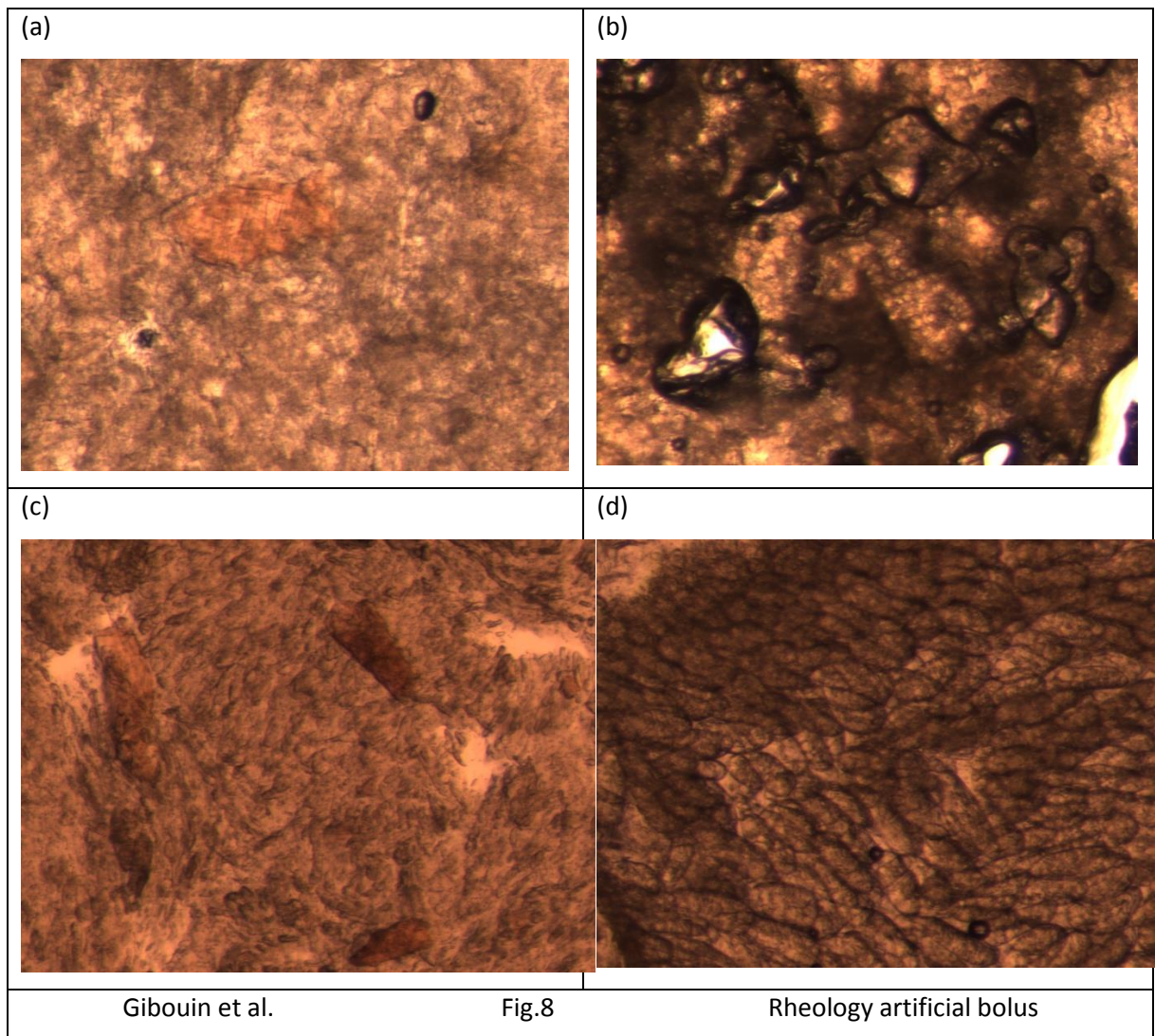


525

526

527

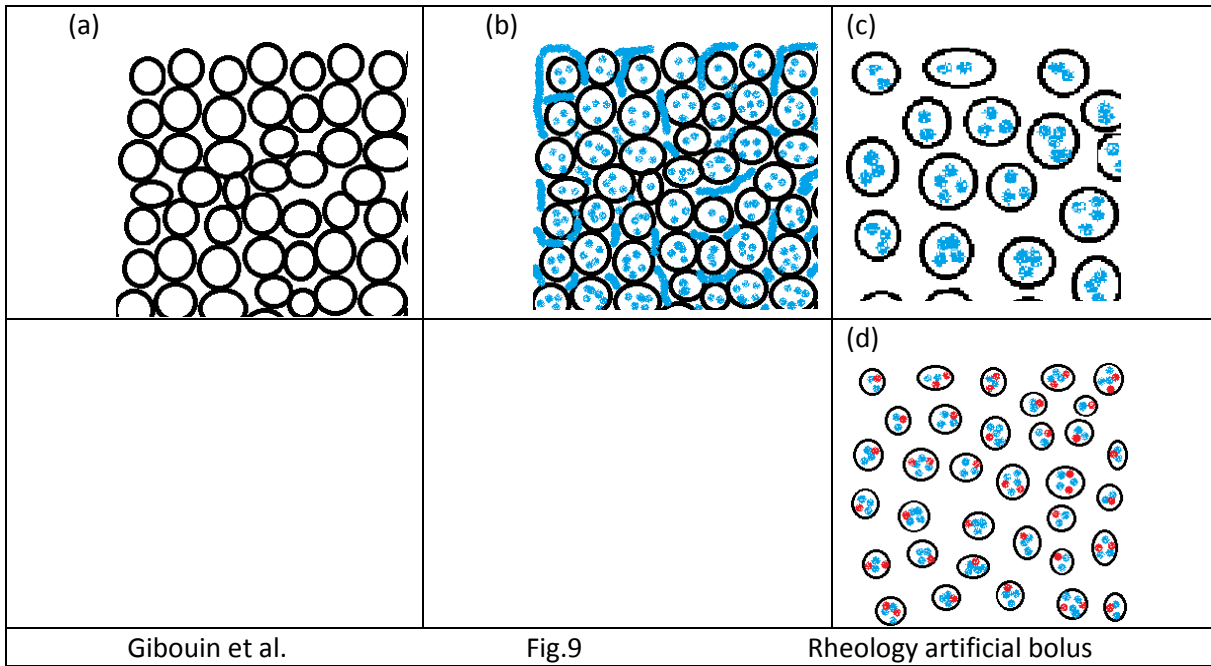
528



529

530

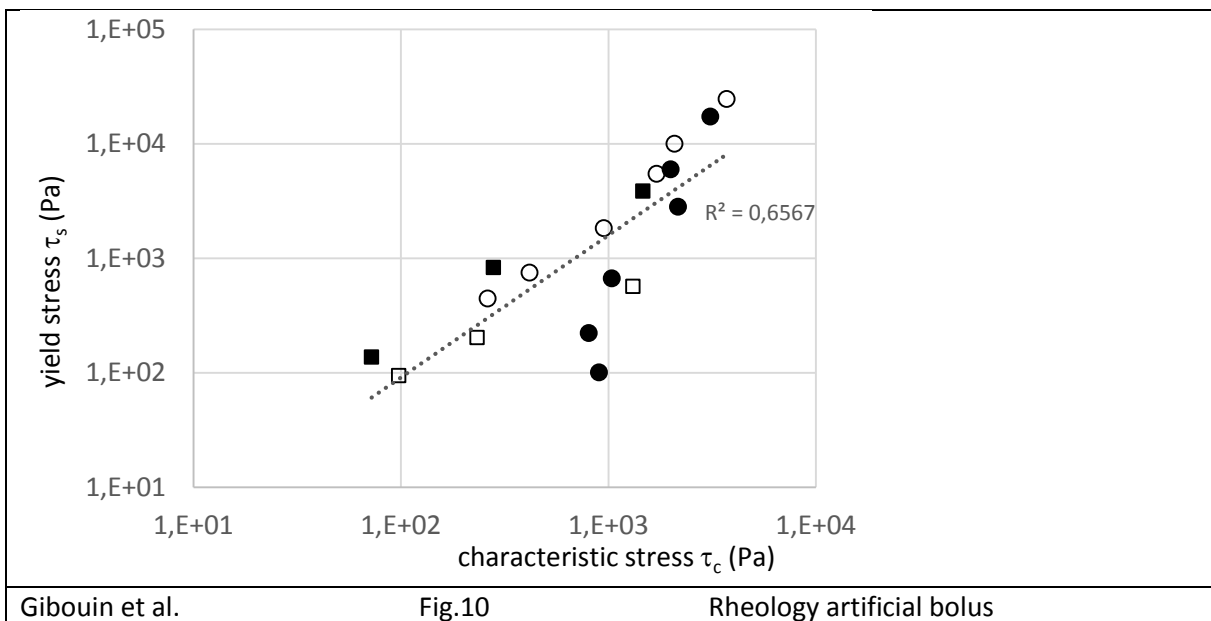
531



532

533

534



535

536

537

538 Table 1: Composition (% total wet basis) and density of the four tested foods, sponge cake (SC) and
 539 extruded (E), and their protein enriched version (SCP and EFP).

Food	Sponge cake		Extruded		
	Code name	SC	SCP	EF	EFP
Protein		11	13	13	23
Fat		6	5	5	-
Starch		18	13	67	42
Sugar		27	26	4	3
Cellulosic compounds (+ others)		10	13	5	22
Water content (% tot. wet mat.)		28	30	5	10
Density (g.cm ⁻³)		0.21	0.23	0.14	0.15

540

541

542 Table 2: Values of the parameters of the models representing the relations between bolus
 543 rheological properties and water content WC (see eqs 1, 3, 6).

Parameter	Viscoelastic domain				Flow regime			
	G' ₀	α _G	τ _{c0}	α _{τc}	τ _{s0}	α _τ	K _{c0}	α _K
Food	MPa		kPa		kPa		kPa.s ⁿ	
SC	2.34	10.4	57.7	9.3	1670	14.4	120	10.4
SCP	0.37	5.5	12	4.8	3190	18.0	1510	14.2
EF	2.6	9.5	5.8 10 ⁵	19.3	4200	13.2	44	7.7
EFP	1.4 10 ⁸	30.8	1.04 10 ⁸	26.5	2.15 10 ⁹	29.5	49110	18

544

545

546 Table 3: Values of Herschel-Bulkley coefficients (see eq. (4)) for each product at chosen reference
 547 value of WC.

Food	WC ref	τ _s (Pa)	K (Pa.s ⁿ)	n
SC	0.54	685	430	0.28
SCP	0.52	270	915	0.21
EF	0.67	985	325	0.41
EFP	0.68	4410	235	0.39

548

549